Bukhtiyarov P.G., Persikov E.S., Shaposhnikova O.Y., Nekrasov A.N. Foundations of the method of complete extraction of metals (Fe, Ni, Co) from rocks and poor ores at moderate hydrogen pressures. (Preliminary results) *UDC 123.456*

IEM RAS. Chernogolovka, pavel@iem. ac. ru

Abstract. The foundations of the original method of almost complete extraction of metals of variable valence (Fe, Ni, Co) from rocks (andesite, basalt, gabbro-norite) have been developed. The technique is based on the experimentally established features of the interaction of hydrogen with melts of such igneous rocks in the hydrogen pressure range of 0.2 - 3 MPa, the temperature range of 1150 - 1300 °C and the duration of the experiments is 1 - 6 hours. It was shown that despite the low oxygen potential in the experiments ($f(O_2) = 10^{-13} - 10^{-14}$), the reduction reaction of metal oxides of variable valence (Fe, Ni, Co) from melts was not fully completed. At the same time, it was found that the main reason for stopping the reduction reactions was water, a product of reduction reactions, which dissolved in melts and thereby increased the oxygen potential. The first successful results were obtained by placing a buffer in the fluid phase – tantalum wire, the oxidation of which led to the decomposition of water in the fluid and the acceleration of the rate of diffusion of water from the melts.

Keywords: gabbro-norite melt, hydrogen, pressure, temperature, metal, reducing conditions

The process of complete reduction of iron oxides with hydrogen from Fe-poor materials (rocks, slags, etc.) is an urgent technological and environmental task. Previous studies on experimental modeling of the formation of native metals in the earth's crust during the interaction of hydrogen with basalt and andesite melts (Persikov et al., 2019; Persikov , Bukhtiyarov , Aranovich 2020; Persikov et al., 2022) showed that despite the low oxygen potential in the experiments ($f(O_2) = 10^{-13} – 10^{-14}$), the reduction reaction of metal oxides of variable valence (Fe, Ni, Co) from melts was not fully completed. At the same time, it was found that the main reason for stopping the reduction reactions was water, a product of reduction reactions, which dissolved in melts, diffused into the fluid phase (initially pure hydrogen), but slower by two orders of magnitude compared to the counter diffusion of hydrogen (Persikov et al., 1990), and thereby increased the potential of oxygen. To accelerate the removal of water from the melts, a multiple cyclic decrease in the pressure of hydrogen in the system in the isothermal mode and tantalum buffer were used. A series of experiments was carried out at low hydrogen pressures ($P(H_2) = 0.2 –3$ MPa) to develop the foundations of the original method for almost complete extraction of metals of variable valence (Fe, Ni, Co) from rocks.

The experiments were carried out with the help of a unique high-gas pressure device equipped with an original internal device, which made it possible to conduct long-term experiments at high temperatures, despite the high penetrating power of hydrogen (Pis.1.). The device includes a molybdenum reactor with a placed in it with an alundum ampoule with the original sample. The reactor is hermetically connected to the piston equalizer - separator. The internal volumes of the molybdenum reactor and the equalizer-separator under the piston were filled with hydrogen at a pressure of 3 MPa using a special system. The device assembled in this way, together with the internal heater, was placed inside a high-pressure vessel in such a way that the ampoule with the sample was in the gradient-free temperature zone of the heater.

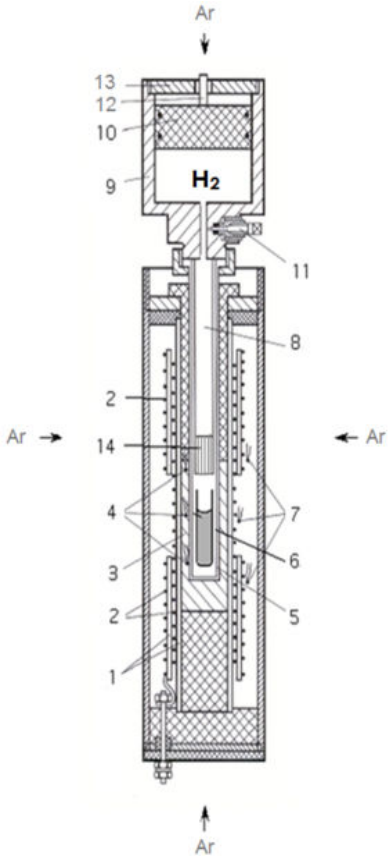

Fig. 1. Scheme of the unique internal device and internal heater of the gas pressure vessel.

1, 3 - insulators; 2 - two windings of the heater; 4 - three thermocouples to control the temperature gradient along the ampoule with the sample; 5 - molybdenum reactor; 6 - alundum ampoule with a sample (melt); 7 - two thermocouples to control the temperature of each heater winding; 8 - sapphire cylinder; 9 - equalizer-separator housing; 10 - equalizer-separator piston; 11 - shut-off valve; 12 - sensor for monitoring the position of the piston; 13 - cover; 14 - alundum ampoule with tantalum wire.

Due to the movement of the equalizer-separator piston, the hydrogen pressure in the internal volume of the molybdenum reactor was always kept equal to the gas pressure (Ar) in the vessel during the experiment. The error in measuring the temperature of the experiment was ± 5°C, and the hydrogen pressure was ± 0.1 % rel. As an initial sample, the gabbro-norite of the Chineysky massif, Transbaikalia was taken (Table 1).

Table 1. Chemical compositions (wt. %) of the initial glass of gabbro-norite and melts (glasses) after experiments under hydrogen pressure

Comp.	№ 2169	№ 2171	№ 2173	Gabbro-norite remelted, (original glass)
SiO_2	44.23	54.10	47.86	44.19
Al_2O_3	18.50	16.32	15.59	12.24
FeO	13.65	1.15	10.89	20.27
MnO	0.20	0.27	0.21	0.21
MgO	6.42	8.07	6.85	6.52
CaO	11.38	13.90	12.36	11.31
Na_2O	1.98	2.39	2.23	1.90
K_2O	0.27	0.32	0.34	0.3
TiO_2	3.37	3.47	3.67	2.66
P_2O_5	0.00	0.07	0	0.12
Sum	100.00	100.00	100.00	100.00

Table 2. Chemical composition (wt.%) of the metal phase in quenched samples of gabbro-norite melt after experiments under hydrogen pressure

Comp.	№ 2169	№ 2171	№ 2173
Fe	99.92	99.49	99.95
Mn	0.08	0.00	0.04
Mg	0.00	0.01	0.00
Ca	0.00	0.11	0.00
Si	0.00	0.09	0.00
Ti	0.00	0.01	0.01
Sum	100.00	99.8	100.00

(a)

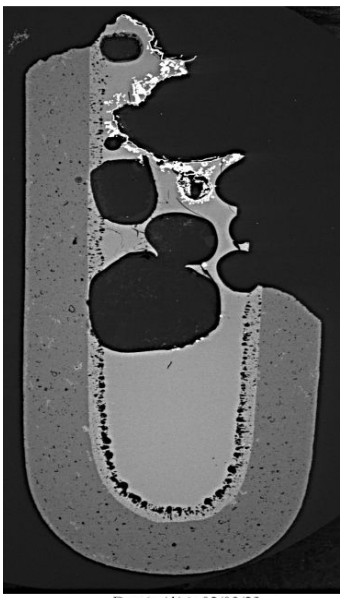

№2169

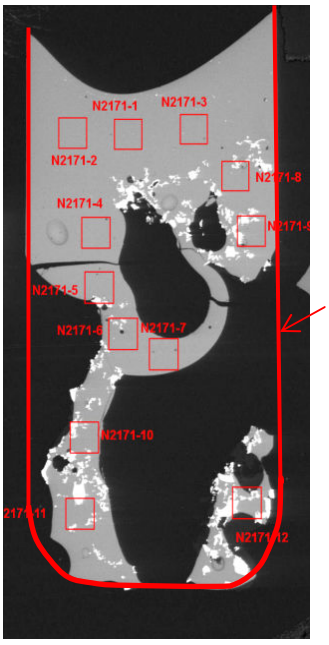

№2171

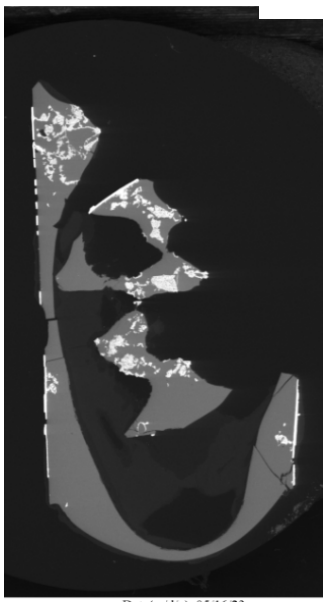

№2173

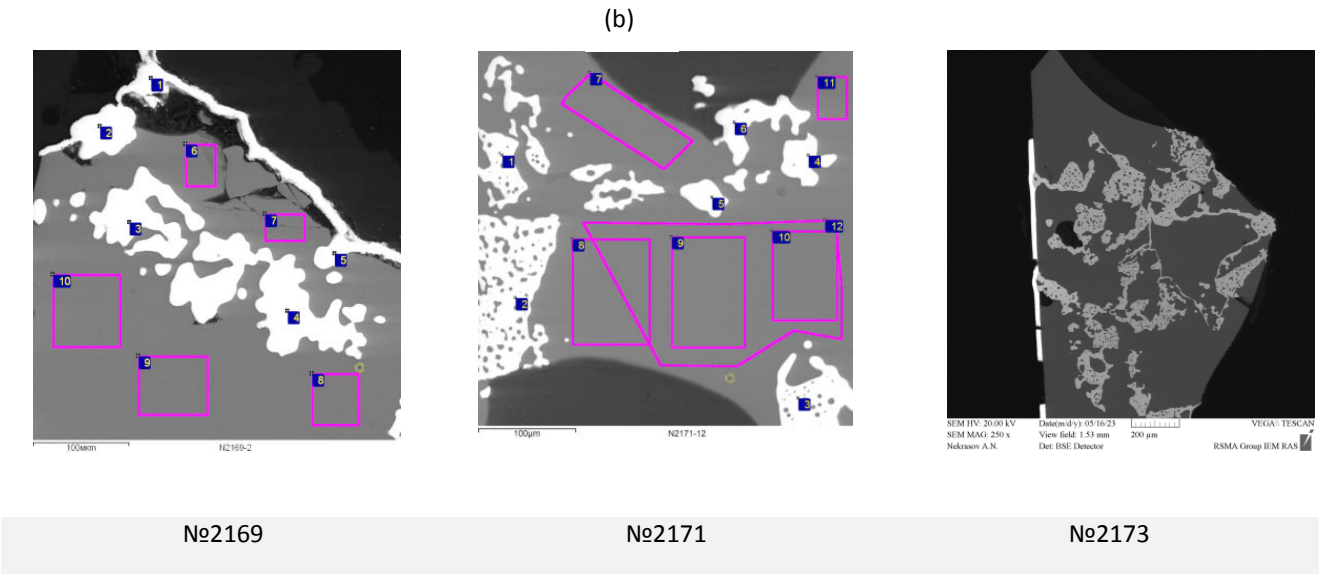

Fig. 2. Raster micrograph in reflected scattered electrons (BSE) quenching samples after experiments on the interaction of gabbro-norite melt with hydrogen. (a) - cross-sections of samples after experiments No. 2169 (alundum ampoule without W foil and Ta buffer with pre-treatment of the sample in the solid state); experiment No. 2171 (alundum ampoule with W foil and Ta buffer in the fluid phase with pre-treatment of the sample in the solid state) and No. 2173 (alundum ampoule with W foil and with Ta buffer without pre-treatment of the sample in the solid state); (b) - separation of the metal phase: gray - silicate glass (see Table 1), white - metal phase (see Table 2).

The experiments were carried out in alund ampoules with a diameter of 6 mm, into the inside of which a thin (0.01 mm thick) W foil was inserted to prevent the melt from interacting with the ampoule. Parameters of the experiments: hydrogen pressure 0.2 – 3 MPa, temperature range 1150 – 1300 ° C, duration of experiments 1 – 6 hours. The experiments were carried out in two stages: 1 - processing of rock without melting it (T = 1150 °C), 2 – melting of rock (T = 1300 °C). Both stages were carried out with a cyclic change in the isothermal regime of hydrogen pressure.

To compare the compositions of tempered and initial melts, gabbro-norite glass was deposited in a high-temperature furnace (T = 1450 °C, exposure 3 hours, Table 1). After isobaric quenching, vessel pressure relief and complete cooling, the internal device was removed from the gas pressure vessel, the ampoule with the sample was removed from the molybdenum reactor for subsequent analysis of the phases formed during the experiment. The chemical composition of the phases obtained in the experiments (Tables 1, 2) was determined using a digital electron X-ray microscope CamScan MV2300 (VEGA TS 5130 MM), with attachment for energy-dispersive microanalysis INCA Energy 450 and WDS Oxford INCA Wave 700. The analyses were carried out at an accelerating voltage of 20 kV with a beam current of up to 400 nA and a spectra-set time of 50-100 seconds. In Fig. 2. aster photographs in reflected scattered electrons (BSE) of quenching samples (a) and micrographs of individual areas with iron (b) separations are presented. As can be seen (see Table 1), the most complete reduction was in experiment No. 2171, where, when hydrogen reacts with a gabbro-norite melt, the Fe content decreases from 20.27 wt. %. to 1.15 wt. %. In other experiments, the separation of iron from the melt was not so significant. In the future, it is planned to improve this technique, aimed at the effective separation of the metal and silicate phases.

The work was carried out within the framework of the research topic No. FMUF-2022-0004 of the IEM RAS with the financial support of the Russian Science Foundation, grant No. 22-27-00124.

References:

E.S. Persikov, P.G. Bukhtiyarov, L.Ya. Aranovich A.N., Nekrasov, O.Yu. Shaposhnikova (2019) Experimental modeling of formation of native metals (Fe,Ni,Co) in the earth's crust by the interaction of hydrogen with basaltic melts. Geohemistry International, Vol. 57, No. 10, pp. 1035–1044.

Persikov E. S., Bukhtiyarov P. G., Aranovich L. Ya. (2020). Features of hydrogen interaction with basaltic melts at pressures 10 – 100 MPa and temperatures 1100 - 1250°C . Chemical Geol., vol. 556, pp. 1-7.

Persikov E.S., Bukhtiyarov P.G., Aranovich L.Ya, Nekrasov A.N., Kosova C.A. (2022) Metal-silicate separation in andesite melts interacting with hydrogen (experimental study). Experiments in GeoSciences, V. 28, № 1, pp. 111-113.

Persikov E.S., Zharikov V.A., Bukhtiyarov P.G., Pol'skoy S.F. (1990) The effect of volatiles on the properties of magmatic melts. Eur. J. Mineral., 2, pp. 621- 642

Kotelnikov A.R., Korzhinskaya V.S., Suk N.I., Novikov M.P., Van K.V. Experimental investigations of solubility of $Zr_{0.5}Hf_{0.5}SiO_4$ solid solution in silicate melts *UDC 550.89*

IEM RAS, Chernogolovka, Moscow district
(kotelnik@iem.ac.ru)

Abstract. The solubility of the $Zr_{0.5}Hf_{0.5}SiO_4$ solid solution in an aluminosilicate melt at temperatures of 800°C and 1000°C, P = 200 MPa, in the presence of water was studied. The duration of the experiments was 12–14 days. In the experiments, we used granite (Orlovka deposit, well 42), preliminarily melted at atmospheric pressure and a temperature of 980°C, as well as $Zr_{0.5}Hf_{0.5}SiO_4$ synthesized by the solution-melt method at T = 1250°C from a stoichiometric mixture of oxides ZrO_2 + HfO_2 + SiO_2, reagent $K_2Mo_3O_{10}$ was used as a flux. Were prepared pre-melted aluminosilicate glass with different agpaity coefficient: Kagp = (Na+K)/Al: from 0.95 to 2.05. The effect of agpaiticity on the solubility of a solid solution in an aluminosilicate melt in the presence of water has been established: with an increase in Kagp from 0.98 to 1.82, the total content of (ZrO_2 + HfO_2) in glass increases on average to 6.35 wt %. It is noted that the agpaiticity of the melt has a stronger effect on the solubility of the $Zr_{0.5}Hf_{0.5}SiO_4$ solid solution than the temperature.

Keywords: silicate melt; solid solution; experiment; solubility

Experimental method The solubility of the $Zr_{0.5}Hf_{0.5}SiO_4$ solid solution in an aluminosilicate melt was experimentally studied at T = 800 –1000°C and P = 200 MPa on a high gas pressure vessel (HGPV-10000) in the presence of water. The duration of the experiments was 12 - 14 days. Starting materials were: granite (Orlovka deposit, well 42) of the following composition (wt %): SiO_2 - 72.10; TiO_2 - 0.01; Al_2O_3 – 16.14; Fe_2O_3 – 0.68; MnO - 0.09; CaO - 0.30; MgO - 0.01; Na_2O - 5.17; K_2O - 4.28; P_2O_5 - 0.02; F - 0.32; H_2O - 0.18, pre-melted at atmospheric pressure and a temperature of 980°C, as well as a solid solution of the composition $Zr_{0.5}Hf_{0.5}SiO_4$, (ZrcHfn), synthesized by us by the solution-melt method at T = 1250°C from a stoichiometric mixture of ZrO_2 + HfO_2 + SiO_2 oxides. As a charge for the synthesis of ZrcHfn, we used ZrO_2 and HfO_2 reagents (high grade) and silicon dioxide SiO_2 (synthetic). Quartz was preheated to 500°C and dipped into distilled water, after which it was ground in an agate mortar to a powder state. The reagent $K_2Mo_3O_{10}$ was used as a flux. The ratio of charge and flux was 1:10. The homogenization time was 5 hours, after which the temperature was reduced at a rate of 5°C per hour to T = 900°C, and then the mixture was gradually cooled to 25°C. The cooled solution-melt mixture was washed with conc. HCl until complete dissolution of potassium molybdate. The charge was washed with H_2O and dried at 100°C. Synthesis products were identified primarily by X-ray, optical and microprobe determinations.

To elucidate the effect of agpaiticity on the solubility of $Zr_{0.5}Hf_{0.5}SiO_4$, preliminarily melted aluminosilicate glasses were prepared with different agpaitic coefficients K_{agp} = (Na+K)/Al: from 0.98 to 2.05. Previously, to assess the solubility of zircon in an aluminosilicate melt, we used a method of measuring the diffusion profile of the ZrO_2 content in quenched glass from the boundary of a zircon crystal (Kotelnikov et al., 2019). It was found that at a distance of ~200 μm from the zircon crystal, the ZrO_2 contents in the glass remain constant and then begin to decrease. This gives grounds to take these maximum values for the solubility of ZrO_2 in the melt. The solubility of the $Zr_{0.5}Hf_{0.5}SiO_4$ solid solution in an aluminosilicate melt was also studied by a similar procedure. The experiments were carried out in gold (800°C) and platinum (1000°C) 3x0.1x50 mm ampoules, which were loaded with 50–80 mg of granite glass, 5–7 mg of the synthesized $Zr_{0.5}Hf_{0.5}SiO_4$ solid solution. A certain amount of water was poured into the ampoules (Tables 1 and 2). The ampoules were hermetically sealed and placed in a "gas" bomb for the experiment. The compositions of all samples after the experiments were determined by electron probe X-ray spectral analysis (EPSSA) using a Tescan Vega II XMU scanning electron microscope (Tescan, Czech Republic) equipped with an INCA Energy 450 X-ray spectral microanalysis system with energy-dispersive (INCAx-sight) and crystal- diffraction (INCA wave 700) X-ray spectrometers (Oxford Instruments, England) and INCA Energy+ software platform.

Experimental results Table 1 presents the results of experiments on the solubility of $Zr_{0.5}Hf_{0.5}SiO_4$ in a melt with different agpaitic values at T = 1000°C, P = 200 MPa. Figure 1a shows the dependence of the solubility of $Zr_{0.5}Hf_{0.5}SiO_4$ in an aluminosilicate melt on the agpaitic coefficient (K_{agp} = (Na+K)/Al) in the presence of water (T = 1000°C, P = 200 MPa, duration 12 days).

It has been established that with an increase in K_{agp} from 1.11 to 1.65, the contents of ∑(ZrO_2 + HfO_2) in glass increase on average from 1.38 wt.% to 5.13 wt.%. The glass composition is as follows (wt %): Na_2O - 7.46; Al_2O_3 – 11.84; SiO_2 - 56.67; K_2O - 7.12; CaO - 0.11; TiO_2 – 0.07; F - 0.05 (for K_{agp} = 1.65). As the agpaitic coefficient increases to K_{agp} = 1.99, the content of ∑(ZrO_2 + HfO_2) in the glass begins to decrease.

After the experiments, the agpaiticity of the melt somewhat decreased compared to the initial value, which can be explained by the partial redistribution of alkalis into the fluid phase.

Table 2 presents the results of experiments on the solubility of $Zr_{0.5}Hf_{0.5}SiO_4$ in a melt with different

agpaitic coefficient at T = 800°C, P = 200 MPa. Figure 1b shows the dependence of the solubility of $Zr_{0.5}Hf_{0.5}SiO_4$ in an aluminosilicate melt on the agpaiticity (K_{agp} = (Na+K)/Al) in the presence of water (the duration of the experiments was 14 days).

For 800°C, with an increase in agpaiticity from 1.12 to 1.82, the total content in glass (ZrO_2 + HfO_2) changes from 0.32 to 6.35 wt.%. For 800°C, the agpaiticity of the melt slightly increased after the experiments. The glass composition for K_{agp} = 1.82 is as follows (wt %): Na_2O - 8.68; Al_2O_3 – 11.17; SiO_2 - 56.43; K_2O - 7.43; CaO - 0.13; TiO_2 - 0.02.

Table 1. Experiments on the solubility of $Zr_{0.5}Hf_{0.5}Si0_4$ in a melt with different agpaiticity T = 1000°C, 200 MPa

№ exp.	Weight, mg	Solution, mg	ZrO_2 wt.%	HfO_2 wt.%	ZrO_2+ HfO_2 wt.%	K_{agp} before exp. K_{agp} after exp.
ZrcHfn-7	83.0gr. + 8.86 $Zrc_{0.5}Hfn_{0.5}$	H_2O – 47.55	0.47	0.91	1.38	K_{agp} bef/ex=1.19 K_{agp} aft/ex=1.11
ZrcHfn-8	81.59gr.+8.33 $Zrc_{0.5}Hfn_{0.5}$	H_2O – 47.57	1.30	3.30	4.60	K_{agp} bef/ex=1.51 K_{agp} aft/ex =1.49
ZrcHfn-10	84.95gr.+8.74 $Zrc_{0.5}Hfn_{0.5}$	H_2O – 41.90	1.45	3.58	5.03	K_{agp} bef/ex=2.05 K_{agp} aft/ex=1.99
ZrcHfn-3	52.59gr.+5.36 $Zrc_{0.5}Hfn_{0.5}$	H_2O – 46.22	0.89	1.03	1.92	K_{agp} bef/ex=1.51 K_{agp} aft/ex=1.15
ZrcHfn-4	50.55gr.+5.52 $Zrc_{0.5}Hfn_{0.5}$	H_2O – 47.53	1.87	2.54	4.41	K_{agp} bef/ex=1.75 K_{agp} aft/ex= 1.44
ZrcHfn-5	50.51gr.+5.74 $Zrc_{0.5}Hfn_{0.5}$	H_2O – 48.51	2.15	2.98	5.13	K_{agp} bef/ex=2.05 K_{agp} aft/ex= 1.65

Note. gr. – granite glass.

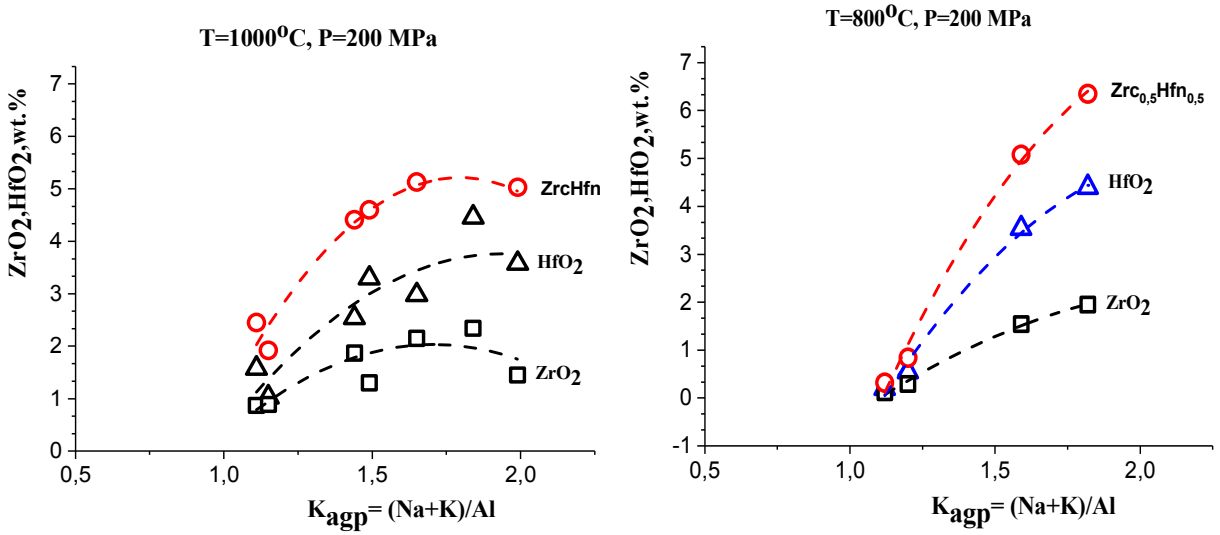

Fig. 1a. Dependence of the solubility of the $Zrc_{0.5}Hfn_{0.5}$ solid solution in the aluminosilicate melt on the agpaiticity in the presence of water (T = 1000°C, P = 200 MPa)

Fig. 1b. Dependence of the solubility of the $Zrc_{0.5}Hfn_{0.5}$ solid solution in the aluminosilicate melt on the agpaiticity in the presence of water (T = 800°C, P = 200 MPa)

Table 2. Experiments on the solubility of $Zr_{0.5}Hf_{0.5}Si0_4$ in a melt with different agpaiticity T = 800°C, 200 MPa

№ exp.	Weigh, mg	Solution, mg	ZrO_2, wt.%	HfO_2, wt.%	ZrO_2+ HfO_2, wt.%	K_{agp} before exp. K_{agp} after exp
ZrcHfn-12	51.40gr.+5.31 $Zrc_{0.5}Hfn_{0.5}$	H_2O – 25.07	0.12	0.20	0.32	K_{agp} bef/ex=1.10 K_{agp} aft/ex =1.12
ZrcHfn-13	53.51gr.+7.13 $Zrc_{0.5}Hfn_{0.5}$	H_2O – 50.27	0.29	0.55	0.84	K_{agp} bef/ex=1.19 K_{agp} aft/ex= 1.20
ZrcHfn-14	55.04gr.+5.64 $Zrc_{0.5}Hfn_{0.5}$	H_2O – 49.72	1.54	3.54	5.08	K_{agp} bef/ex=1.51 K_{agp} aft/ex= 1.59
ZrcHfn-15	54.26gr.+5.36 $Zrc_{0.5}Hfn_{0.5}$	H_2O – 50.32	1.95	4.10	6.35	K_{agp} bef/ex=1.75 K_{agp} aft/ex= 1.82

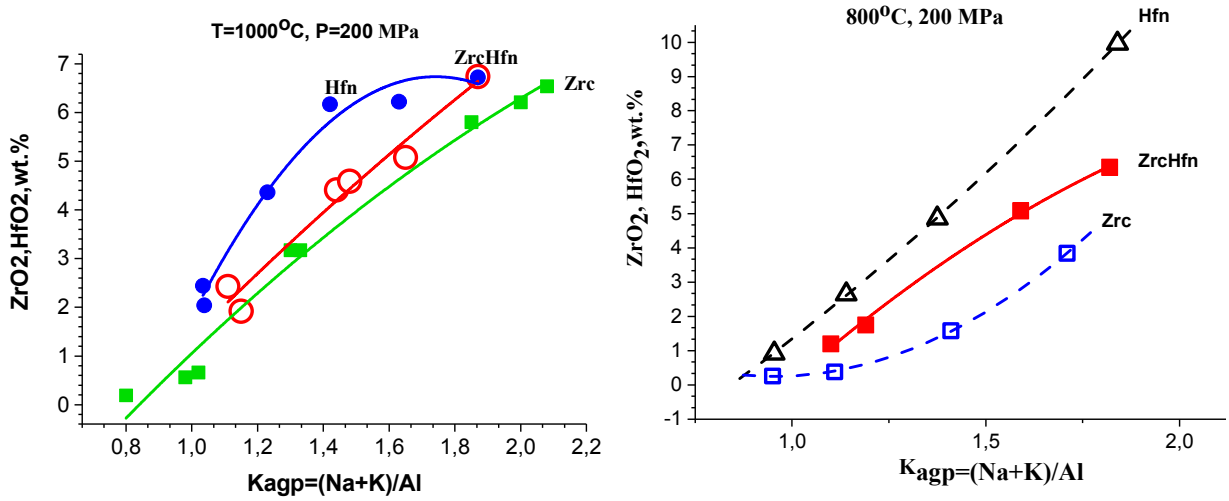

Fig. 2a. Solubility curves of zircon (Zrc), hafnon (Hfn) and $Zrc_{0.5}Hfn_{0.5}$ solid solution in silicate melt versus agpaiticity (K_{agp}= (Na+K)/Al in the presence of water. (T=1000°C, P=200 MPa)

Fig. 2b. Solubility curves of zircon (Zrc), hafnon (Hfn) and $Zrc_{0.5}Hfn_{0.5}$ solid solution in silicate melt versus agpaiticity (K_{agp} = (Na+K)/Al in the presence of water. (T=800°C, P=200 MPa)

Figures 2a and 2b show for comparison the dependence curves of the zircon (Zrc), hafnon (Hfn), and solid solution (ZrcHfn) solubility for T = 1000°C (Fig. 2a) and 800°C (Fig. 2b) at P = 200 MPa. It can be seen that the solubility of hafnon in the melt in the presence of water is higher than the solubility of zircon (Kotelnikov et al., 2020) and higher than the solubility of the solid solution (ZrcHfn), whose solubility occupies an intermediate position.

As a result of the research, it was found that the agpaiticity of the melt has a stronger effect on the solubility of these minerals than temperature.

The work was supported by the FMUF-2022-0004 program.

References

Kotelnikov A.R., Korzhinskaya V.S., Suk N.I., Van K.V., Virus A.A. Experimental study of zircon and loparite solubility in silicate melt // Experiment in Geosciences. 2019, V. 2. N 1. P. 138 - 140. (ISSN: 0869-2904).

Kotelnikov A.R., Korzhinskaya V.S., Suk N.I., Van K.V. Experimental study of zircon and hafnon solubility in silicate melts // Experiment in Geosciences. 2020. V. 26. N 1. P. 155-158. (ISSN: 0869-2904.).

Shchekina T.I.[1], Rusak A.A.[2], Zinovieva N.G.[1], Alferyeva Ya. O.[1], Kotelnikov A. R.[3] Distribution of thorium and uranium between silicate and salt alkali-aluminum-fluoride melts in a granite system at 700 °C and 800 °C and 1 kbar *UDC 552.11*

[1]Lomonosov Moscow State University (MSU), Faculty of Geology, Moscow,
[2]Vernadsky Institute of Geochemistry and Analytical Chemistry of the Russian Academy of Sciences (GEOKHI RAS), Moscow,
[3]Korzhinsky Institute of Experimental Mineralogy of the Russian Academy of Sciences, Chernogolovka, Moscow district (kotelnik1950@yandex.ru)

Abstract. The distribution of Th and U between aluminosilicate and LiKNa-aluminofluoride (salt) melts in the Si-Al-Na-K-Li-F-O-H model granite system at 800°C and 700°C and 1 kbar was studied. It is shown that at 800°C thorium and uranium are distributed in favor of a salt melt compared to an aluminosilicate melt. However, the separation coefficients between them for Th are significantly higher than those for U. It was found that the solubility of U and Th in the aluminosilicate and salt melt equilibrium with it depends on the composition of the system and is greatest in the presence of Li, Na and K. At 700°C, a cryolite-like phase crystallizes from the salt melt, in which Th and U are practically not included. Both elements accumulate in the residual salt melt, which occupies the gaps between cryolite single crystals in the salt phase. The Th content in the residual salt melt is 5-10 wt. %. U is mainly included in the silicate melt. Phases such as torite, solid solutions of the thorianite-uraninite series, and Th and U fluorides crystallize at the boundary of the two melts. The accumulation of actinoids in the salt melt under experimental conditions at 800°C and their isolation as their own minerals at 700°C explains the presence of thorium and uranium minerals in rare metal

cryolite-containing granites and their pegmatites. It is assumed that ore concentrations of Th and U occur even at the magmatic stage of the formation of rare-metal granites.

Keywords: aluminosilicate, LiKNa-aluminofluoride, salt melts, solubility, thorium, uranium, rare-metal granites.

Uranium and thorium are among the most common and widely used radioactive elements of the actinide family, which determines the significant similarity of their chemical properties. They are close to the lanthanide group, which is important for the geochemistry of uranium and thorium. In terms of ionic radii, U^{4+} is closer to the group of "heavy" lanthanides (yttrium group), while Th^{4+} is closer to the group of "light" ones (cerium group). Due to the similarity of actinides and lanthanides, many rare earth minerals contain variable amounts of uranium and thorium in the form of isomorphic impurities. Due to the closeness of the ionic radii and the equality of charges between U^{4+} and Th^{4+}, the identity of their chemical properties is manifested. In endogenous minerals, where uranium is tetravalent, U and Th often form isostructural series, for example: UO_2 (uraninite) ↔ ThO_2 (thorianite), $USiO_4$ (coffinite) ↔ $ThSiO_4$ (thorite).

The behavior of uranium and thorium in the Si-Al-Na-K-Li-H_2O-F granite system under conditions of its saturation with water and fluorine at temperatures of 700–800°C, a pressure of 1000 bar and a water content of 4 to 10 wt. %. The experiments were carried out on a high-pressure hydrothermal installation with external heating and on a high-pressure gas installation with internal heating in platinum ampoules. The fugacity of oxygen in the experiments corresponded to the NNO buffer. Temperature control accuracy was ± 5°C, pressure ± 100 bar. The duration of the experiments was from 5 to 7 days.

Dried gels of stoichiometric composition $NaAlSi_3O_8$, $KAlSi_3O_8$, SiO_2, reagents $NaAlO_2$, Al_2O_3, AlF_3, NaF, KF, LiF, K_2SiF_6, Na_3AlF_6 were used as starting materials for preparing the charge. When studying the distribution of elements, U and Th were introduced into the charge in the amount of 1 and 2 wt. %: uranium in the form of metal, thorium in the form of ThO_2.

To diagnose phases and determine their composition in relation to rock-forming elements, fluorine and oxygen, a Jeol JSM-6480LV scanning electron microscope (Jeol, Japan) with an Oxford X-MaxN energy-dispersive spectrometer (Oxford Instrument Ltd., Great Britain), purchased at the expense of Development programs of Moscow University, in the laboratory of local research methods of the Department of Petrology and Volcanology, Faculty of Geology, Moscow State University. Electronic images of the sample structure, phase morphology, and phase relations were received in the mode of reflected electrons (BSE). Analysis of the contents of Si, Al, Na, K, F, U, and Th was also carried out on a Camebax-SX 50 electronic microanalyzer of the Department of Mineralogy, Moscow State University. Shooting mode: voltage E_0 = 20 kV, exposure τ = 10 sec, current I = 30 nA. UO_2 and $ThSiO_4$ were used as standards for U and Th analyses. Typically, the analysis was carried out by scanning over the area of the analyzed phase. At least 3 - 5 determinations of the composition of each phase were carried out. The limit of determination of uranium and thorium is about 0,01%, the error in most samples is about 30 rel.%. The lower limit of fluorine determination is 0,05%, the relative error is ±2%. CaF_2, LiF, MgF_2, LaF_3 were used as standards in the analysis of fluorine. The instrumental error in measuring fluorine was ±2% of the element concentration. The contents of Li in the phases of the experiments in the reference compositions were previously determined by the method of n-α radiography (Gramenitsky et al., 2005), or approximately estimated from the deficit of the analysis amount. The contents of U and Th and water in some experiments were determined using an ion microprobe. According to these data, the solubility of water in all studied compositions was 5-8 wt.%.

In this work, we consider the distribution of thorium and uranium between silicate and salt melts in the Li-containing part of the system at temperatures of 800 and 700°C. The distribution of these elements between the aluminosilicate melt and cryolite (Crl), which is a liquidus mineral in a system saturated with fluorine, was previously studied by us (Gramenitsky et al., 2005) in the Na-, Na-K, and K quartz-normative and nepheline-normative parts of the system. It was found that uranium and thorium are predominantly concentrated in the aluminosilicate melt (up to 0,5%).

Upon transition to the Li-containing part of the system, a fundamental change in phase relations was found in the area of sodium, sodium-potassium and potassium quartz-normative aluminosilicate melts (Shchekina et al, 2021). In the original compositions, sodium and potassium were replaced by an equivalent atomic amount of lithium. Starting from the atomic fraction of lithium 0,1 in the system of the sum (Li + K) and 0,25 of the sum (Li + Na), the phase relations in the system change dramatically due to the manifestation of aluminosilicate-aluminofluoride immiscibility. In equilibrium with the aluminosilicate melt (L) at 800°C, there are not crystals of aluminofluorides, but a fluoride melt (LF), similar in composition to $(Li,Na,K)_3AlF_6$.

The aluminosilicate melt contains from tenths to

2,5 wt.% of dissolved lithium (depending on the initial concentration of Li in the mixture), and in other components differs little from the melt obtained in similar experiments without lithium. Alumofluoride melt forms globular or ellipsoidal discharge (globules) up to several mm in size (Fig. 1a). They consist of an aggregate of quenching crystals of aluminum, sodium, potassium and lithium fluorides (Fig. 1b). In some experiments, silica-containing glass was found among the quenching phases. Such a structure of globules in lithium-containing experiments leaves no doubt that they are formed from a fluoride melt. The behavior of U and, especially, Th also changes dramatically, since they begin to concentrate mainly in the salt melt with separation coefficients significantly greater than one. Fig.1b shows that LF salt globules are enriched with Th and U, where they are represented (in BSE) by the smallest quenching phases. At the contact of LF with the aluminosilicate melt, larger crystals are formed, usually composed of uraninite UO_2 with an admixture of thorium.

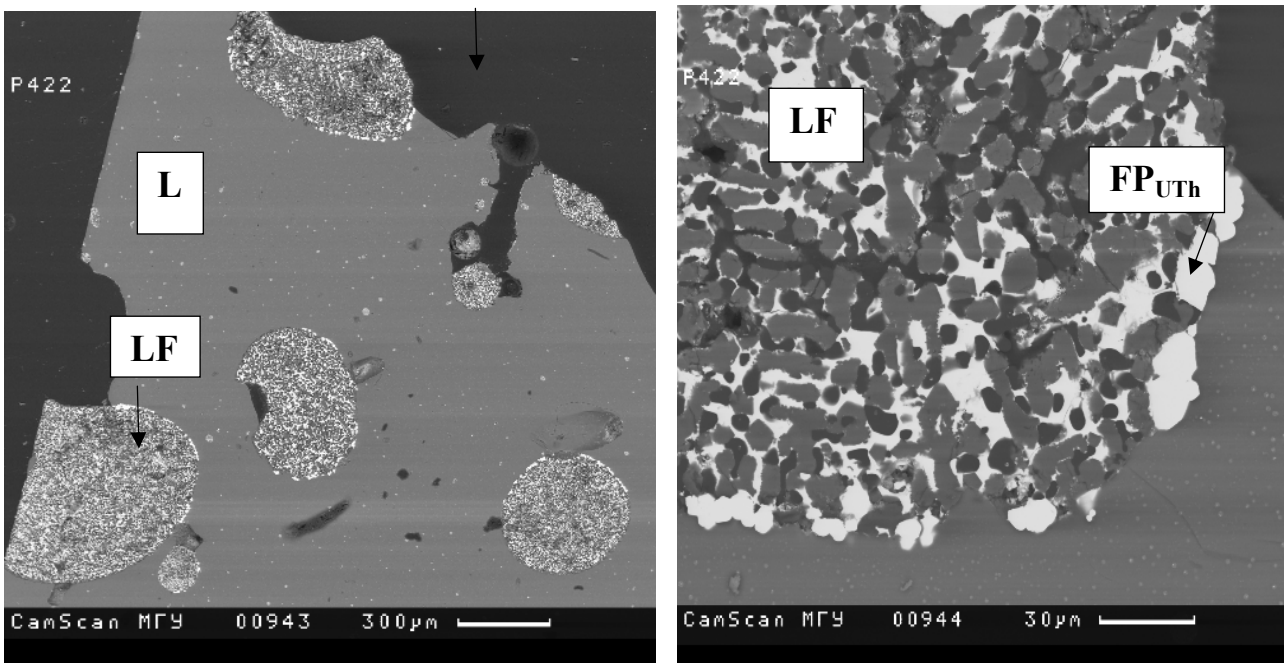

a *b*

Fig. 1. Phase relations in a granite system with water, fluorine and lithium (in BSE): a-globules of salt melt LF in aluminosilicate glass L; b – quenching phases of salt globule LF with FP LiKNa – cryolite (gray); drops of LiF (black); FP_{UTh} – oxides and fluorides U and Th (white).

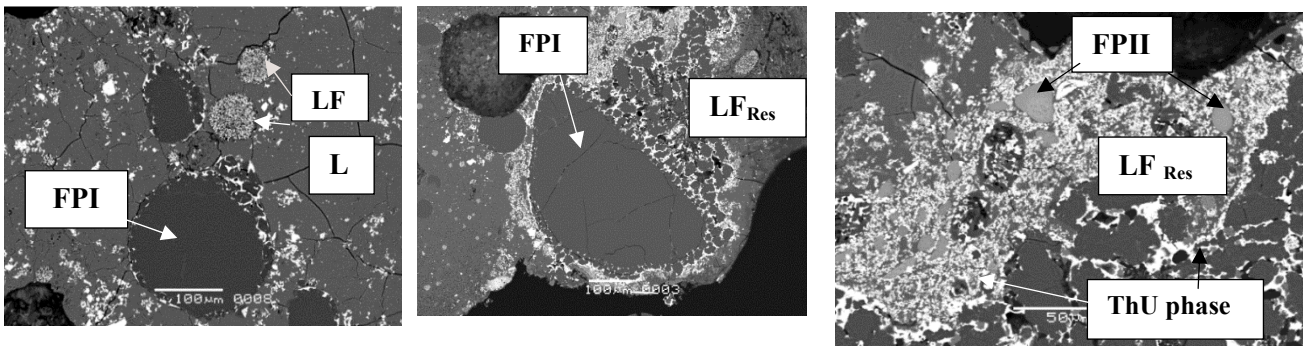

a *b* *c*

Fig.2 (a, b, c). Phase relations, types and morphology of salt phase secretions in samples at 700°C, 1 kbar (L-aluminosilicate melt, LF – salt melt, LREs – residual salt melt in a globule, FPI – crystalline cryolite phase, FPII – KNa(Li) phase containing Th and U, the white phases in BSE are oxides and fluorides of Th and U).

When the temperature of the experiment decreases to 700°C, the phase relations change due to the crystallization of the salt phase inside large globules of the salt melt (Fig. 2a-c). Under an electron microscope, it can be seen that salt globules of three types are observed in the sample material composed of ~80% silicate glass. The largest of them (type I FP) have a size from 10 to 500 microns and are composed of single crystals of KNa-cryolite, which fill most of the space of the former globule (Fig. 2a). In their composition, there is a sharp predominance of Na over K (almost 10 times) and an F/Al ratio of about 6 (5,7), close to cryolite. In total, the analyses of this phase have a deficit of about 6,3 wt.%. It is assumed that this crystalline phase may contain Li. This phase does not contain U and Th. But at its border with silicate glass, fringes from ore mountains of phases (white) enriched with U are always observed, as was the case in experiments at 800 °C.

Table 1. Partition coefficients between salt and aluminosilicate melts for Th, Y, LREE, HREE, Sc and U.

LogKD(LF/L)	Th	Y	LREE	HREE	Sc	U
Li-Na-K	1,92	1,45	1,44	1,33	0,90	0,59

Part of the material of FP type I globules is fragmented along the edges, divided into oval or irregular-shaped secretions, between which rounded black secretions are observed with a length of 5 to 29 and a width of up to 5-7 microns (apparently, LiF melt) and U-Th ore material of white color. The residual salt melt L_{RES} enriched with Li is pushed to the boundaries of the globule. It consists of quenching phases of fluorides and alkaline aluminofluorides of light gray color (in the SSE mode), having a teardrop shape (FP type II). This phase consists of alumofluoride with a small (~1.5 times) predominance of K over Na and contains up to 12 wt.% Th, and does not contain U (Fig. 2 in). The third type of globules (LF) (Fig. 1a) is represented by rounded and oval segregation of no more than 50 microns in size, consisting of many quenching phases of gray and white color. The appearance of these LF globules is closest to what we are familiar with from previous experiments with Li-containing alkaline-aluminum fluoride phases at 800°C (Fig. 1a). It can be said that the phase is characterized by a 4-fold predominance of Na over K and a ratio of F/Al= 6-7. Apparently, it was a melt that dissolved quite a lot of ore up to 11 mass.% Th and up to 0.8 mass.% U. Analyses also show a deficiency in the amount, possibly caused by the presence of Li in the globules, which has not been analyzed. Within the sample, uraninite crystallized directly from aluminosilicate glass composition $U_{0,96-0,98}$, $Th_{0.04-0.02}$.

Within the globules of the salt phase, among the quenching ore phases, thorite, thorianite, and Th- and U-fluoride containing Na and K. The partition coefficients between salt and aluminosilicate melts were compared with previously obtained similar data (Gramenitsky et al., 2005) for REE, Y, and Sc (Table 1).

When considering the behavior of uranium and thorium in comparison with the data previously obtained for scandium, yttrium, light and heavy rare earth elements under the same conditions and compositions of the system, a number of decreases in the affinity of elements to a salt Li-containing fluoride melt were obtained: Th →Y→LREE→HREE →Sc →U (Fig. 3).

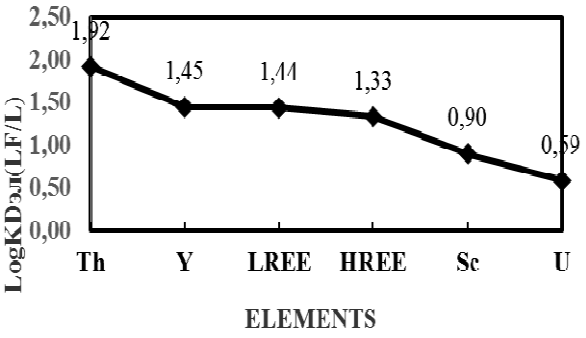

Fig.3.

Conclusion. It was found that the difference in the behavior of U and Th, despite the proximity of their chemical properties, consists in a stronger affinity of thorium to fluoride melts compared to other phases in the system. Differences in the partition coefficients and the increased (compared with uranium) solubility of thorium in salt melts in a lithium-containing granite system lead to differences in the behavior of these elements and to a change in U/Th ratios. Such a difference can manifest itself during the differentiation of granitic magma at its most recent stages, for example, during the formation of pegmatites and cryolite-containing granites. The appearance of liquid immiscibility in fluorine- and lithium-rich magmas may enhance differences in the behavior of uranium and thorium, especially for potassium-enriched compositions.

The work was carried out on the state budget topic "Modes of petrogenesis of the Earth's internal geospheres" of the Geological Faculty of Lomonosov Moscow State University, with the support of the state assignment of GEOKHI RAS and IEM RAS and with the financial support of the RFBR grant (project № 16-05-0089).

References

Gramenitsky E.N., Shchekina T.I., Devyatova V.N. Phase relations in fluorine-containing granite and nepheline-syenite systems and the distribution of elements between phases. M.: GEOS. 2005. 186 p.

Shchekina T.I., Rusak A.A., Alferyeva Y.O., Kotelnikov A.R., Zinovieva N.G., Khvostikov V.A. Behavior of lithium in the liuidus part of a high-fluorine granite system at pressures from 100 to 500 MPa // ISSN 0145-8752, Moscow University Geology Bulletin, 2021, Vol. 76, № 4, pp. 423–435. © Allerton Press, Inc., 2021.

Suk N.I., Kotelnikov A.R. Wolframite solubility in aluminosilicate melt *UDC 550.89*

IEM RAS, Chernogolovka Moscow district,
(sukni@iem.ac.ru; kotelnik@iem.ac.ru)

Abstract. Experimental study of the solubility of wolframite (Fe,Mn)WO4 in aluminosilicate melts of different alkalinity at T = 1100°C and P = 1 and 4 kbar under dry conditions and in the presence of 10 wt. % H_2O revealed its dependence on the agpaiticity ((Na+K)/Al) of the melt. At T = 1100°C and P = 1 kbar, the solubility of wolframite increases with an increase in the agpaiticity of the melt. At P = 4 kbar, the content of tungsten in aluminosilicate glass increases significantly, but the opposite pattern is observed: the content of WO3 in the melt decreases with an increase in its agpaitic coefficient, which is associated with the formation of crystals of alkaline tungsten compounds. In water-containing systems, melt heterogeneity is observed in the form of emulsion formation, which is expressed in the presence of microscopic droplets enriched in tungsten.

Keywords: wolframite, aluminosilicate melt, experiment

The solubility of wolframite (Fe,Mn)WO_4 in aluminosilicate melts of different alkalinity at T = 1100°C and P = 1 and 4 kbar was experimentally studied under dry conditions and in the presence of 10 wt. %H_2O. The experiments were carried out on a high gas pressure vessel. The duration of the experiments was 5 days. The initial material was melted glass of granite composition with different agpaitic values (0.9–2), as well as natural wolframite. The composition of the samples after the experiments was determined by the method of electron probe X-ray spectral analysis.

As a result of the experiment, a column of glass with wolframite crystals was obtained. After the experiments, the agpaiticity of the melt decreased compared to the initial value, which is explained by the partial redistribution of alkalis into the fluid phase. It was found that at T = 1100°C and P = 1 kbar, the solubility of wolframite depends on the composition of the aluminosilicate melt (Fig. 1), slightly increasing with increasing melt agpaiticity ((Na+K)/Al). At K_{agp}=1.02, the content of WO_3 is 1.61 wt.%, and at K_{agp}=1.26 it increases to 2.04 wt.%. The resulting dependence can be quite well described by the equation:

y = 2.80567*exp((-0.17946)/(X-0.69688)), where X=(Na+K)/Al.

At P=4 kbar, the solubility of wolframite in aluminosilicate glass increases significantly, but the opposite pattern is observed: the WO_3 content in the melt decreases with an increase in its agpaitic coefficient (Fig. 1). This is due to the appearance of newly formed crystals, the composition of which corresponds to the alkaline compounds of tungsten (sodium and potassium tungstates). In this case, at least three phases coexist: the melt, wolframite crystals, and sodium and potassium tungstates, the amount of which increases with an increase in the agpaiticity of the melt, which decreases compared to the initial one. The dependence of the solubility of wolframite in the melt for these parameters can be described by the equation:

$y = \exp(6.58903+(-7.69689)*X+(2.72693)*X^2)$, where X=(Na+K)/Al.

In water-containing systems, melt heterogeneity was observed in the form of emulsion formation, expressed in the presence of microscopic droplets enriched in tungsten. At 4 kbar, the emulsion formation is most pronounced (Fig. 2). Sometimes during hardening, apparently, partial crystallization occurs with the formation of microcrystals. Due to this, the WO_3 content in the melt increases significantly (up to ~5 wt.% at 1 kbar, and up to ~12 wt.% at 4 kbar). Such a melt can be considered as ore-bearing.

Probably, this phenomenon is similar to the titanate-silicate liquid immiscibility obtained earlier (Suk, 2007, 2012, 2017) in water-containing aluminosilicate systems containing ore elements (Ti, Nb, Sr, REE).

To find out the composition of the resulting emulsion droplets, experiments were carried out in the aluminosilicate melt – Na_2WO_4*2 H_2O system at T = 1100°C and P = 1 and 4 kbar. After the experiment, crystals of practically pure sodium tungstate with an insignificant admixture of potassium were observed in the sample, which formed a layer in the lower part of the glass column,

and drops were present in the glass, which also corresponded in composition to alkaline (sodium) tungstate with an insignificant admixture of potassium, calcium, and aluminum (Fig. 3). This suggests that the composition of the emulsion drops is similar.

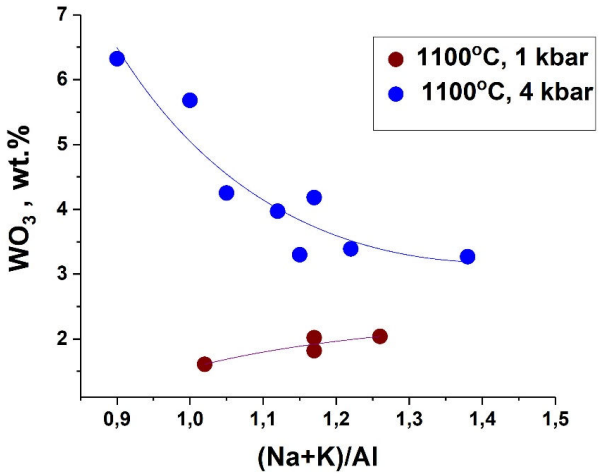

Fig. 1. Solubility of wolframite in the melt obtained at T=1100°C and pressures of 1 and 4 kbar.

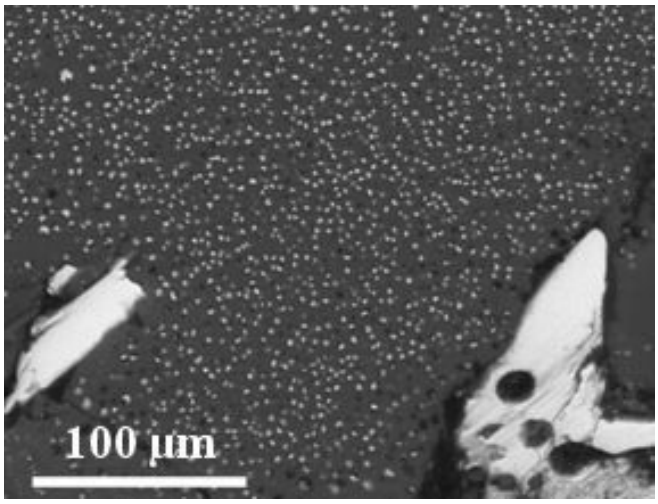

Fig. 2. Formation of an emulsion in equilibrium with wolframite crystals in water-containing systems at T=1100°C and P=4 kbar.

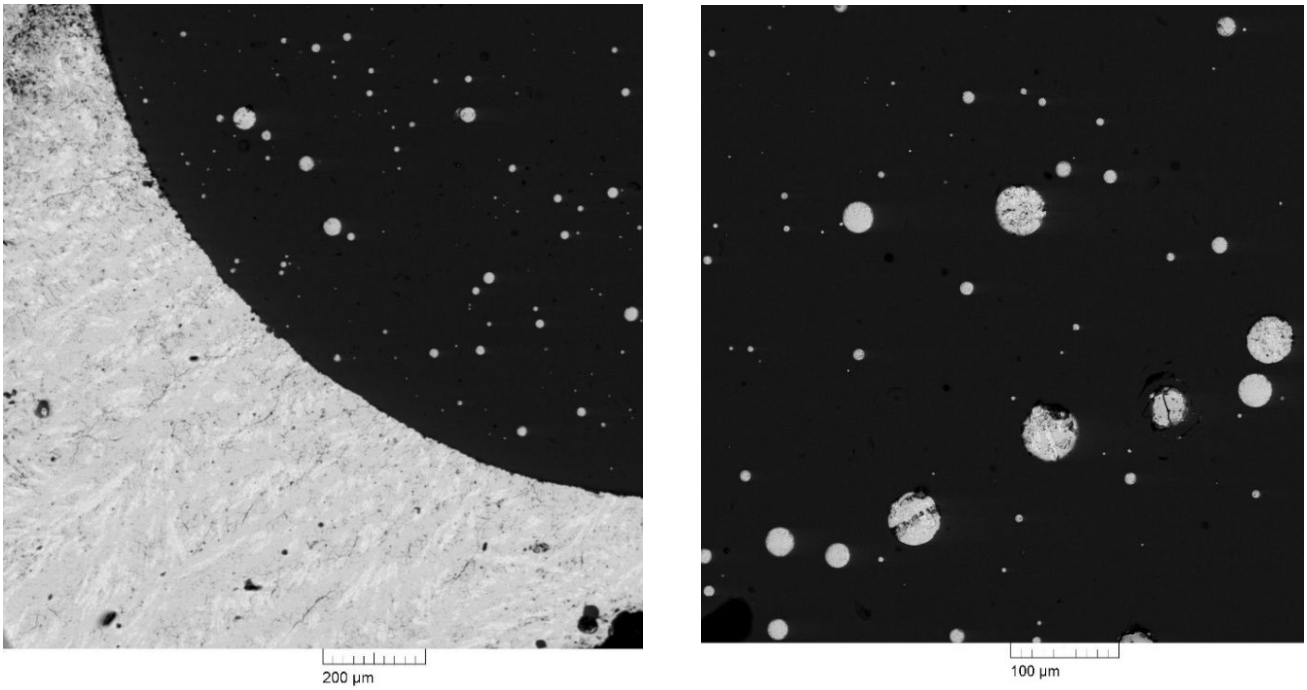

Fig. 3. Crystalline layer and droplets of alkaline (sodium) tungstate obtained in the aluminosilicate melt – Na_2WO_4*2 H_2O system at T = 1100°C and P = 4 kbar.

The work was supported by the FMUF-2022-0004 program.

References

Suk N.I. Experimental study of alkaline magmatic aluminosilicate systems: implication for the genesis of REE-Nb loparite deposits. V. 414. No 1. P. 615-618.

Suk N.I. Experimental study of liquid immiscibility in the fluid-magmatic silicate systems containing Ti, Nb, Sr, REE, and Zr. Petrology. 2012. V. 20. N 2. P.138-146.

Suk N.I. Liquid immiscibility in alkaline magmatic systems. 2017. M.: “KDU”, “University book”, 238 p.

Suk N.I., Kotelnikov A.R., Viryus A.A. Features of loparite dissolution in aluminosilicate melts *UDC 550.89*

IEM RAS, Chernogolovka Moscow district,
(sukni@iem.ac.ru; kotelnik@iem.ac.ru)

Abstract. The solubility of loparite in aluminosilicate melts of various compositions was experimentally studied at T=1200 and 1000°C and P=2 kbar under dry conditions and in the presence of 10 wt.% H2O in a high gas pressure vessel with a duration of 1 day. The initial material was previously melted glasses of malignite, urtite and eutectic albite-nepheline composition, as well as natural loparite of the Lovozero massif. The dependence of the solubility of loparite on the composition of the aluminosilicate melt (Ca/(Na+K), (Na+K)/Al) has been revealed. Partition coefficients of a number of elements between silicate melt and loparite crystals (Ki=Cimelt/Cilop) were estimated.

Keywords: experiment, loparite, aluminosilicate melt

The solubility of loparite in aluminosilicate melts of various compositions was experimentally studied at T=1200 and 1000°C and P=2 kbar under dry conditions and in the presence of 10 wt.% H_2O in a high gas pressure vessel with a duration of 1 day. The starting material was synthetic glasses of malignite, urtite and eutectic albite-nepheline composition, preliminarily deposited at T=1450°C in a furnace with lanthanum-chromite heaters in platinum crucibles for 2 hours, as well as natural loparite $(Na,Ce,Ca)_2(Ti,Nb)_2O_6$) of the Lovozero massif.

The compositions of the samples after the experiments were determined on a Tescan Vega II XMU scanning electron microscope (Czech Republic) equipped with energy dispersive (INCAx-sight) and crystal diffraction (INCA wave) X-ray spectrometers (England, Oxford). The program for qualitative and quantitative analysis INCA Energy 450 was used. Samples were analyzed using both energy dispersive (for the main rock-forming elements) and crystal diffraction (for Sr, Nb, La, Ce, Nd) spectrometers.

Experimental results. After the experiments, glass with loparite crystals was observed in the sample. During the experiments, the aluminosilicate melt was saturated with elements characteristic of loparite. At the same time, in the malignite melt at T=1200°C and P=2 kbar, the formation of rims on loparite crystals was observed, differing in composition from loparite (Fig. 1a). In the rims, the contents of Na_2O, SrO, Nb_2O_5, and, to a lesser extent, TiO_2 decrease. Due to this, the relative content of rare earth elements increases. This indicates that Ti, Na, Sr, and Nb migrate from loparite to the alkaline melt more easily than REE. In water-containing systems, the rim is better expressed than in dry systems.

This is also evidenced by estimates of the partition coefficients of elements between loparite crystals and the melt (C_i^{melt}/C_i^{lop}, where C is the concentration of oxides in wt %). For more correct calculations, we used the values obtained as a result of recalculating the analyzes of glasses for dry systems by 100 wt.%, and the analyzes of water-containing glasses for systems of albite-nepheline composition by 95 wt.%. In the melt of malignite and albite-nepheline compositions at T = 1000°C and P = 2 kbar, the average values of the partition coefficients for TiO_2 are the same (0.067), while for SrO they differ insignificantly: 0.315 (in the melt of the malignite composition) and 0.328 (in the melt of the albite-nepheline composition), respectively.

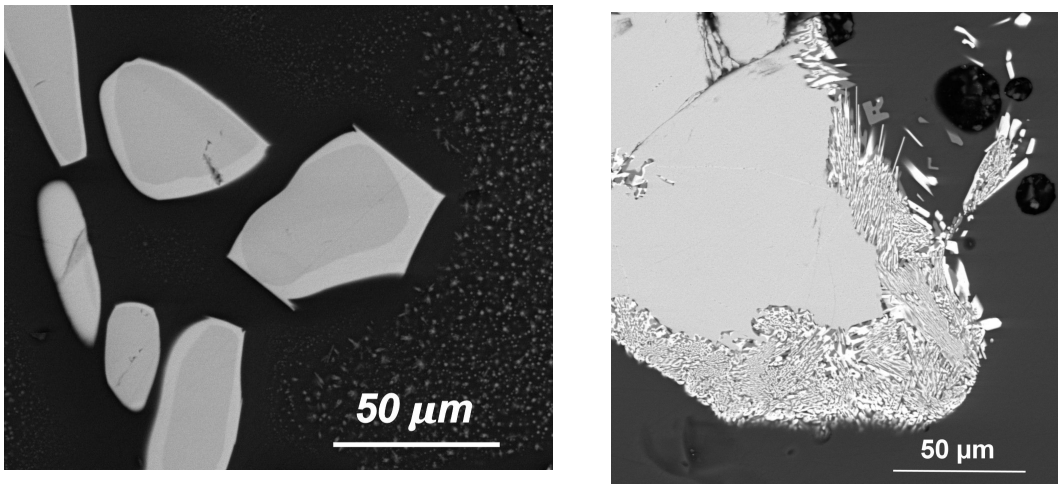

a *b*

Fig. 1. Rims formed on loparite crystals in experiments with malignite melt (a) and the formation of rare earth titanosilicate crystals around loparite grains in a melt corresponding to the composition of Ab-Ne eutectic (b) at T=1200°C and P=2 kbar.

For Nb_2O_5, La_2O_3, Ce_2O_3 and Nd_2O_3, the average partition coefficients are much lower in experiments with a melt corresponding to the composition of albite-nepheline eutectic: K_{Nb2O5} = 0.039(0.080), K_{La2O3} = 0.024(0.045), K_{Ce2O3}=0.023(0.043), K_{Nd2O3}=0.022(0.053). Values for experiments with malignite melt are given in parentheses.For experiments with an urtite melt, the partition factors for La, Ce, and Nd oxides are close to the values in melts corresponding to the composition of the albite-nepheline eutectic (0.018, 0.016, and 0.017, respectively), the partition coefficients for TiO_2 (0.038) and SrO (0.276) are smaller, and for Nb_2O_5 it is greater (0.057) than for melts corresponding to the composition of albite-nepheline eutectic.

At T=1200°C and P=2 kbar, a similar regularity is observed. The average values of partition coefficients decrease in melts corresponding to the composition of albite-nepheline eutectic: K_{TiO2} = 0.071(0.103), K_{SrO} = 0.112(0.122), K_{Nb2O5} = 0.052(0.092), K_{La2O3} = 0.006(0.013), K_{Ce2O3} = 0.023(0.051), K_{Nd2O3} = 0.016(0.039). Values for experiments with malignite melt are given in parentheses.

In the melt, whose composition corresponds to the albite-nepheline eutectic, the formation of crystals of rare earth titanosilicates (Fig. 1b), and sometimes rare earth titaniumoniobates growing on loparite crystals, was observed. Apparently, the formation of such crystals, as well as rims around loparite grains, may indicate incongruent dissolution of loparite in melts.

The solubility of loparite can be estimated by determining the sum of oxides of elements inherent only to loparite (TiO_2, Nb_2O_5, SrO, La_2O_3, Ce_2O_3, Nd_2O_3) in the glass obtained as a result of the experiment. The presence of water had practically no effect on the solubility of loparite. According to the estimates, the solubility of loparite in a melt of malignite composition at T=1000°C and P=2 kbar averages ~ 6 wt.%, in a melt corresponding to the composition of albite-nepheline eutectic, on average ~ 5.3 wt.%, and in a melt corresponding to composition of urtite ~ 3.7 wt.%. At T = 1200°C and P = 2 kbar, in a malignite melt, this value averages ~6.7 wt.%, and in a melt corresponding to the composition of the albite-nepheline eutectic, ~4.6 wt.%. Such values of solubility are insufficient to explain the content of loparite in the malignite horizon, which is associated with rich loparite ores of the Lovozero alkaline massif. The content of loparite in malignite reaches 20-25%. The data obtained can explain the presence of only accessory loparite in the rocks.

It has been established that the solubility of loparite depends on the composition of the aluminosilicate melt: it increases with an increase in the agpaiticity of the melt ((Na+K)/Al) and with an increase in the Ca/(Na+K) ratio. In order to make a more correct comparison, the compositions of the obtained experimental glasses were recalculated into formulas in terms of 50 oxygen atoms. Figure 2 shows the dependences of the contents of elements inherent in loparite on the composition of the aluminosilicate melt. The contents ∑(RE+Ti) = (Ti+Nb+Sr+La+Ce+Nd) in glass slightly increase with increasing temperature. The contents of titanium and niobium (Fig. 3) in the melt behave similarly, increasing with increasing temperature. The contents of ∑REE= (La+Ce+Nd) in glass at 1000°C and in dry systems at 1200°C are practically the same, but they decrease in hydrous melts at 1200°C (Fig. 4). This is probably due to the more intense formation of rare earth titanosilicates.

In water-containing systems, the formation of a microemulsion was constantly observed, expressed in the presence of small droplets enriched in elements characteristic of loparite. Apparently, this is a manifestation of titanate-silicate liquid immiscibility, which was obtained earlier (Suk, 2007, 2012, 2017) in water-containing aluminosilicate systems containing ore elements (Ti, Nb, Sr, REE). The presence of the emulsion made it difficult to analyze the glasses whose compositions were determined in the purest regions of the melt.

Thus, the obtained experimental data show that rich loparite ores cannot be formed by direct crystallization of loparite from the melt. Their formation can only be explained by the occurrence of titanate-silicate immiscibility, as a result of which the magmatic melt is significantly enriched in ore components.

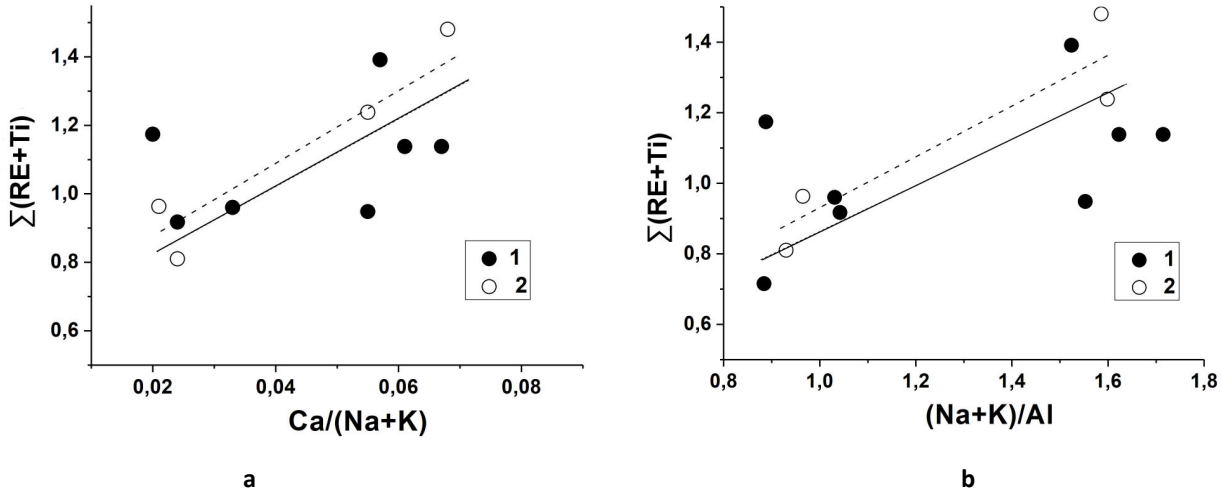

Fig. 2. Dependence of loparite solubility on Ca/(Na+K) of aluminosilicate melt (a) and on agpaiticity ((Na+K)/Al) of aluminosilicate melt (b). ∑(RE+Ti) = Ti+Nb+Sr+La+Ce+Nd, form. units. 1 – T=1000°C, 2 kbar; 2 – T=1200°C, 2 kbar.

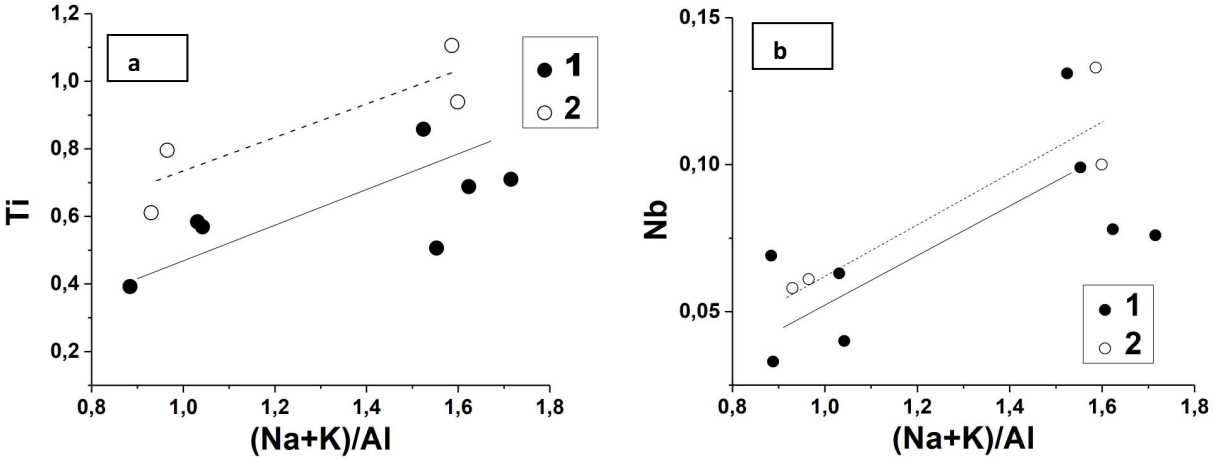

Fig. 3. Dependence of the contents of titanium (a) and niobium (b) on the agpaiticity ((Na+K)/Al) of the aluminosilicate melt (form. units). 1 – T=1000 °C, 2 kbar; 2 – T=1200 °C, 2 kbar.

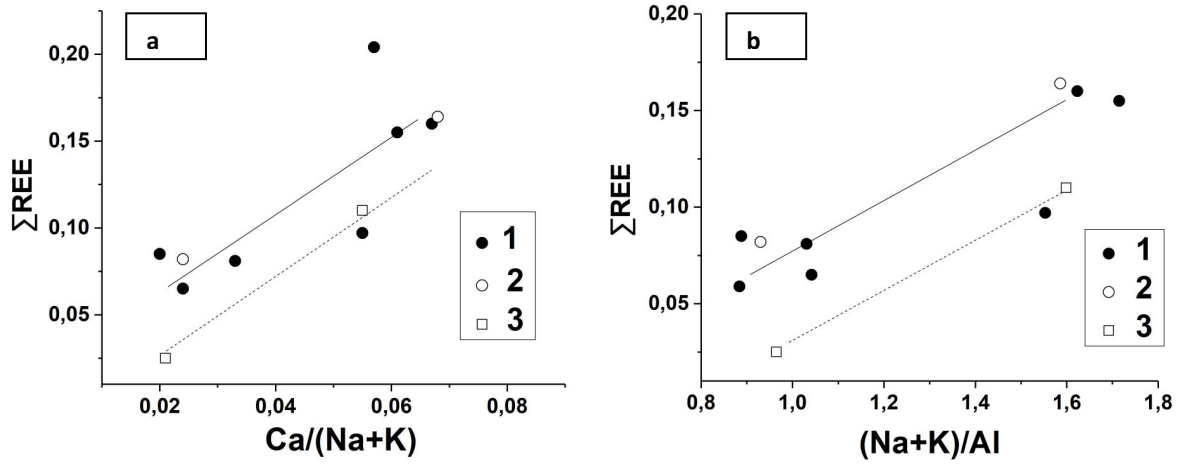

Fig. 4. Dependence of the contents of the sum of rare earth elements (∑REE) on Ca/(Na+K) of the aluminosilicate melt (a) and on the agpaiticity ((Na+K)/Al) of the aluminosilicate melt (b) (form. units). 1 – T=1000°C, 2 kbar; 2 – T=1200°C, 2 kbar (dry systems); 3 – T=1200°C, 2 kbar (water containing systems).

The work was supported by the FMUF-2022-0004 program.

References

Suk N.I. Experimental study of alkaline magmatic aluminosilicate systems: implication for the genesis of REE-Nb loparite deposits. V. 414. No 1. P. 615-618.

Suk N.I. Experimental study of liquid immiscibility in the fluid-magmatic silicate systems containing Ti, Nb, Sr, REE, and Zr. Petrology. 2012. V. 20. N 2. P.138-146.

Suk N.I. Liquid immiscibility in alkaline magmatic systems. 2017. M.: "KDU", "University book", 238 p.

Chevychelov* V.Y., Viryus A.A. On the dissolution of Ta-Nb minerals in granitoid melts *UDC 550.42*

D.S. Korzhinskii Institute of Experimental Mineralogy of Russian Academy of Sciences (IEM RAS)
chev@iem.ac.ru*, allavirus@yandex.ru

Abstract. Experimental data are presented on the contents of Ta and Nb in acid magmatic melts of various alkalinity and alumina content during the dissolution of Ta-Nb minerals: columbite, tantalite, pyrochlore, microlite, ilmenorutilite, ferrotapiolite and loparite at T =650–850°C and P =100–400 MPa, as well as the results of the partitioning of Ta and Nb in the mineral - melt system. Upon dissolution of pyrochlore in melts of granitoids at P =100 MPa and T =650–850°C, the highest content of Nb (0.7–1.9 wt.%) was obtained in alkaline melts, it decreases to ~0.1–0.4 wt.% in subaluminous and peraluminous melts. An increase in temperature increases the solubility of pyrochlore. It has been established that in alkaline and subaluminous melts, decrease in pressure from 400 to 100 MPa does not significantly affect the dissolution of microlite and pyrochlore, while in peraluminous melt, the contents of Ta and Nb decrease by approximately 1.5 times with decrease in pressure. In peraluminous granitoid melt, microlite is stable, while pyrochlore becomes unstable.

Keywords: dissolution; Ta-Nb minerals; granitoid melts; pyrochlore; microlite; experiment

The report presents experimental data on the contents of Ta and Nb in acid magmatic melts of various alkalinity and alumina content during the dissolution of Ta-Nb minerals: columbite, tantalite, pyrochlore, microlite, ilmenorutilite, ferrotapiolite and loparite at T =650 -850°C and P =100 –400 MPa, as well as the results of the partitioning of Ta and Nb in the mineral - melt system.

Model haplogranitoid melts (SiO_2-Al_2O_3-Na_2O-K_2O) with additions of CaO-LiF and mol. $Al_2O_3/(Na_2O+K_2O)$ ratios ~0.64, ~1.10 and ~1.70 were used in the experiments. The following natural minerals were also used: columbite $(Mn,Fe)(Nb,Ta,Ti,Sn)_2O_6$, tantalite $(Mn,Fe)(Ta,Nb,Ti)_2O_6$, pyrochlore $(Ca,Na,La,Ce)(Nb,Ti)O_6F$, OH,Ca-microlite $(Ca,Na,Bi,Mn,Mg)(Ta,Nb,Ti,Fe)(O,OH)_{5.7}F_{0.3}$, ilmenorutile $(Ti,Nb,Fe^{3+})O_2$, ferrotapiolite $Fe^{2+}(Ta,Nb)_2O_6$, Nb-bearing loparite $(Na,Ce,La,Ca,Nd)(Ti,Nb)O_3$ containing ~21-25 wt.% Nb_2O_5.

When preparing the experiments, aluminosilicate glass powder was poured into a Pt capsule, a rather large mineral fragment was placed in the center, 4–40 wt. % of 0.1 N HF solution was added, and the capsule was welded shut. The experiments were carried out in "Internally heated pressure vessel" (IHPV) at T = 650, 750 and 850°C, P = 100 and 400 MPa and duration from 4 to 10 days depending on T and P. The preparations were prepared from the obtained samples for X-ray spectral electron probe analysis (EPMA). Such analysis was carried out along profiles perpendicular to the contact of crystal melted into glass. As a result of processing these analyses, the solubilities of minerals in granitoid melts at the studied conditions were calculated, namely, the maximum concentrations of Nb, Ta (Ce, La) in melts directly at the contact with the mineral (Table 1).

Table 1. Maximum contents of Ta, Nb (wt.%) and Nb/Ta ratios in various granitoid glasses (melts) after experiments on the dissolution of ferrotapiolite, columbite, tantalite and microlite at T = 750°C and P = 100 MPa.

Mineral, run number	Nb/Ta in the mineral	A/NKC or A/NKMF [1]	N_{prof} [2]	Nb [3]	Ta [3]	Nb/Ta in the melt
Ferrotapiolite, PM-24	0.08	0.67	3	0.06	0.93	0.07
		1.15	3	0.02	0.35	0.06
		1.60	3	0.03	0.41	0.08
Columbite, G-8	2.69	0.69	4-9	3.43	1.80	1.91
		1.51	2	0.39	0.24	1.63
		2.08	2	0.05	0.14	0.36
Tantalite, TM-3	0.75	0.52	4	2.32	3.35	0.69
		1.08	4	0.39	0.87	0.45
		1.67	3	0.04	0.38	0.11
Microlite, PM-17	0.05	0.67	3	0.03	0.73	0.04
		1.11	3	0.01	0.17	0.08
		1.66	3	0.02	0.39	0.05

[1] A/NKC or A/NKMF are the molar ratios of $Al_2O_3/(Na_2O+K_2O+CaO)$ and $Al_2O_3/(Na_2O+K_2O+MnO+FeO)$ in granitoid glasses after the experiment. [2] The number of analyzed profiles. [3] The concentrations were obtained using a wave spectrometer. The analysis errors ranged from 0.02 to 0.30 wt.% depending on the *T-P-X* parameters (in the confidence interval P = 0.95). At low contents, the errors are minimal. The contents of Nb in the analyses of microlite and ferrotapiolite are close to the error of the analysis.

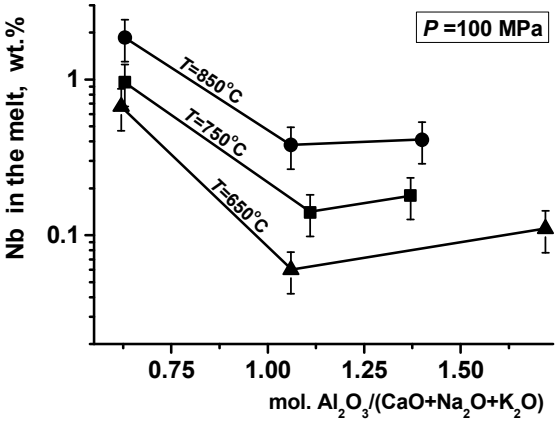

Fig. 1. Temperature dependences of Nb contents in granitoid melts with different alkalinity-alumina content at dissolution of pyrochlore.

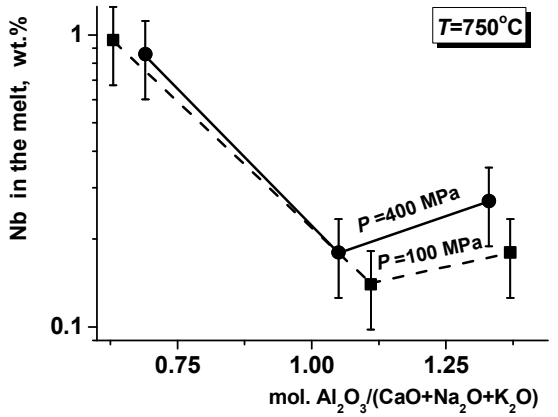

Fig. 2. Concentrations of Nb in the melt at the dissolution of pyrochlore in acid aluminosilicate melts with different alkalinity-alumina content (P = 100 and 400 MPa).

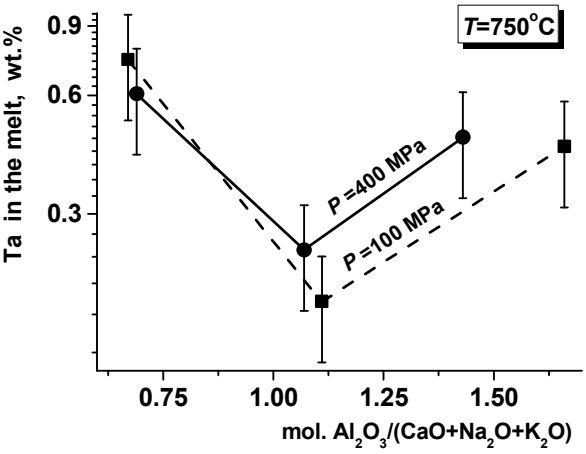

Fig. 3. Concentrations of Ta in the melt at the dissolution of microlite in acid aluminosilicate melts with different alkalinity-alumina content (P = 100 and 400 MPa).

At dissolution of pyrochlore (Fig. 1) in melts of granitoids at P = 100 MPa and T = 650–850°C, the highest content of Nb (0.7–1.9 wt.%) was obtained in the alkaline melt; it decreases to ~0.1–0.4 wt.% in subaluminous and peraluminous melts. An increase in temperature increases the solubility of pyrochlore, and increase in pressure has an ambiguous effect. It has been established that, in alkaline and subaluminous melts, decrease in pressure from 400 to 100 MPa does not significantly affect the dissolution of microlite and pyrochlore, while in peraluminous melt, the contents of Ta and Nb decrease by approximately 1.5 times with a decrease in pressure (Figs. 2 and 3). The results suggest the possibility of deposition of these minerals at high-temperature conditions directly from magmatic melts enriched in alumina and volatile components. In peraluminous granitoid melt, the microlite is stable, while pyrochlore becomes unstable.

It has been shown that ilmenorutile and ferrotapiolite are stable in peraluminous melts, ilmenorutile is also stable in subaluminous and at 650 °C in alkaline melts, and loparite is unstable in all melts studied. The dependences of the content and partitioning of Nb at the dissolution of ilmenorutile and loparite are similar to each other and to those at the dissolution of columbite and tantalite. While the dependences obtained at the dissolution of ferrotapiolite are similar to those obtained at the dissolution of microlite and pyrochlore.

Two types of dependences of the partition coefficients of Nb between the melt and the mineral at the dissolution of minerals in granitoid melts can be distinguished. Group I: columbite, tantalite, ilmenorutile and loparite; Group II: pyrochlore, microlite and ferrotapiolite (Fig. 4). The partitioning of Ta and Nb in these two groups of minerals differ markedly at alkaline melts, the differences between them decrease at subaluminous melts, and at peraluminous melts the partition coefficients of Nb for all studied minerals become close. With increase in aluminium saturation index (A.S.I. = mol. Al/(Na+K+Ca)), the dependences of the first type are characterized by a significant decrease in the partition coefficient of Nb in the entire range of the studied melt compositions, while for the dependences of the second type, this coefficient changes to a lesser extent. This coefficient decreases from alkaline to subaluminous melt, and then it begins to slightly increase with the transition to peraluminous composition.

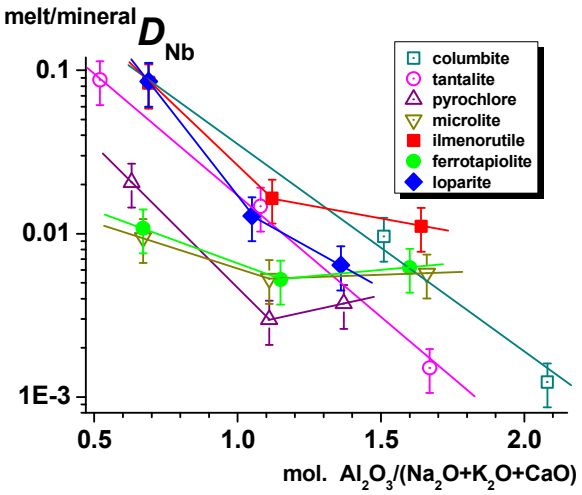

Fig. 4. Partitioning of Nb between granitoid melts and various Nb- and Ta-Nb- minerals depending on the alkalinity -alumina content of the melt at T =750°C and P =100 MPa. Data on the dissolution of loparite were obtained at T =850°C and P =100 MPa.

The Nb/Ta ratios in the melt at the dissolution of ferrotapiolite and microlite are low (from 0.04 to 0.08), close to each other and do not show a clear dependence on the alkalinity - alumina content of the melt (Table 1). When dissolving columbite and tantalite, the Nb/Ta ratios in the melt are 1–1.5 orders of magnitude higher. With increase in the alumina content of the melt, they significantly decrease from 1.9 to 0.4 and from 0.7 to 0.1, respectively, which is associated with higher affinity of Ta for the granitoid melt relative to Nb, especially in peraluminous melts. Comparison of the Nb/Ta ratios in minerals and in melts shows that when columbite and tantalite are dissolved, these ratios in the melt are always lower than in the mineral.

Acnowledgments. The authors thank I.V. Pekov and N.V. Chukanov for kindly providing mineral samples.

Funding. This study was carried out under government-financed research project of IEM RAS No. FMUF-2022-0004 and FMUF-2022-0003.

Chevychelov V.Y. On the dissolution of tantalite in model acidic and alkaline melts

UDC 550.42

D.S. Korzhinskii Institute of Experimental Mineralogy of Russian Academy of Sciences (IEM RAS);
chev@iem.ac.ru

Abstract. Experimental data on the solubility of tantalite in water-saturated granitoid melts with different contents of alumina and alkalis at T = 650 -850°C and P = 100 MPa are presented. It is shown that the maximum Ta content in the melt is always higher than the Nb content. When the composition of the melt changes from alkaline to enriched in Al_2O_3, the contents of Ta and Nb decrease by 1–2 orders of magnitude. At the same time, the Nb/Ta ratio decreases significantly (from ~0.8–0.7 to ~0.4–0.1). This effect is enhanced with decreasing temperature. Therefore, it is likely that it is in alumina-enriched granite melts that a decrease in temperature can lead to a significant separation of Ta and Nb. In this case, in the process of crystallization, Nb will go into mineral phases, while Ta will remain in the melt until the last. It is shown that the effective solubility of Ta in the melt is practically independent of the composition of the dissolving mineral in the columbite-tantalite series. At the same time, the effective solubility of Nb changes significantly.

Keywords: dissolution; tantalite; acidic and alkaline granitoid melts; experiment

The diffusion technique used in the experiments consisted in the dissolution of a mineral (tantalite) in the melt (tantalite was the source of components diffusing into the melt) and subsequent microprobe determination of the composition of the near-contact zone of the melt. The method consists in measuring the contents of the components along the diffusion profiles of dissolution in the melt. These profiles are located perpendicular to the mineral - melt boundary. The dissolution of tantalite in the granitoid melt is limited by diffusion processes, due to the rather low diffusion coefficients of Ta and Nb. The existence of a melt - mineral contact ensures the constancy of the concentrations of diffusing components at the boundary. At constant P-T conditions, as long as the crystalline phase exists, the composition of the melt at the boundary does not change significantly and corresponds to the composition of the liquidus on the state diagram of the system granite melt - dissolved mineral. The resulting diffusion profiles were approximated using exponential equations, and then the limiting concentrations of Ta, Nb, Mn, and Fe in the melt directly at the boundary with the mineral were calculated, which correspond to the effective solubility of these components in the melt.

The composition of initial tantalite from granite pegmatites of Bolivia was the following (wt. %): 10.5MnO, 6.6FeO, 42.9Ta_2O_5, 37.9Nb_2O_5, 1.7TiO_2, 0.4SnO_2.

Table 1. Chemical compositions, molar ratios, and normative compositions of model fluid-saturated acidic and alkaline granitoid melts

wt. %, norm. to 100 %	SiO_2	Al_2O_3	Na_2O	K_2O	A/NK[1]	N/K[1]	SiO_2, mol.%	*Qz*[2]	*Ab*[2]	*Or*[2]	*Ns*[2]	*Crn*[2]
Alkaline melt (*Grn*-0.64)	75.11	11.87	7.92	5.11	0.64	2.36	80.7	29.2	32.6	30.2	8.0	-
Subaluminous melt (*Grn*-1.10)	73.56	16.14	6.27	4.03	1.10	2.36	80.2	21.7	53.1	23.8	-	1.5
Peraluminous melt (*Grn*-1.70)	72.85	19.22	4.83	3.11	1.70	2.36	80.2	32.9	40.9	18.4	-	7.9

[1] A/NK – aluminium saturation index = mol. $Al_2O_3/(Na_2O+K_2O)$. N/K – mol. Na_2O/K_2O.
[2] End-member indexes: Qz—quartz, Ab—albite, Or—orthoclase, Ns—sodium silicate (in real rocks, aegirine and Na-amphiboles), Crn—corundum (in real rocks, topaz).

The main experiments on the study of the solubility of tantalite in model fluid-saturated granitoid melts were carried out in "Internally heated pressure vessel" (IHPV) at T =650, 750 and 850°C (error up to ±5°C) and P =100 MPa (error up to ±1 MPa). When preparing the experiments, 2–3 mg of 0.2 N HF solution was poured onto the bottom of the capsule so that the melt remained fluid-saturated at the experimental conditions. Then glass powder was poured, inside which the tantalite crystal fragment was placed, as if making a "sandwich": glass - mineral - glass. The weight ratio of solution/(glass + mineral) was 0.03–0.07. The poured mixture was compacted, the capsule was purged with Ar and welded shut, controlling each stage by precision weighing with an accuracy of 10^{-5} g. During the experiment, the glass powder melted, and tantalite was dissolved in the aluminosilicate melt by diffusion. The experiments were carried out in welded shut Au capsules, their duration was 3-7 days depending on the temperature.

The change in alkalinity - alumina content ($Al_2O_3/(Na_2O+K_2O+MnO+FeO)$ =A/NKMF index) in the composition of the model granitoid melt has a significant effect on the effective solubility of Ta and Nb (Fig. 1a-c). In alkaline melt, the solubility is maximum and at T =850°C reaches ~4.3 wt.% Ta and ~3.0 wt. % Nb, in subaluminous melt it decreases by 4-5 times to ~1.1-1.0 wt. % Ta and ~0.6 wt. % Nb; and finally in the peraluminous melt the solubility decreases by another factor of 2–3 to ~0.4–0.5 wt. % Ta and ~0.2 wt. %Nb. Note that, with decrease in the content of oxides of alkaline elements and increase in alumina (increase in A/NKMF index), the content of Nb in the melt decreases noticeably faster than Ta. As a result, the difference between the contents of Ta and Nb increases. So on the left in Fig. 1a–1c (in the alkaline melt), the Ta and Nb lines are located side by side, and on the right side on these figures (in the peraluminous melt), they noticeably diverge. Correspondingly, the Nb/Ta ratio in the melt also changes. At the same time, since the content of tantalum in tantalite is higher than niobium, the Nb/Ta ratio is always less than 1 and varies from ~0.8 -0.6 in alkaline melt to ~0.6 -0.1 in subaluminous melt and ~0.45 -0.07 in peraluminous melt. The contents of Mn and Fe in the melts also decrease with change in the composition of the melt from alkaline (~1.1 -0.6 wt.% Mn and ~2.1 -1.0 wt.% Fe) to subaluminous (~0.6 -0.2 wt.% Mn and ~1.0 -0.4 wt.% Fe) and peraluminous (~0.4 -0.2 wt.% Mn and ~0.4 -0.2 wt.% Fe).

The temperature dependence of the solubility of tantalite is positive, but it is weakly pronounced than the composition dependence, especially for Ta. The temperature dependence is most pronounced for the subaluminous melt, in which, as the temperature decreases from 850 to 650°C, the maximum Nb content decreases from ~0.6 to ~0.05 wt. %, and Ta from ~1.1 to ~0.4 wt. %. With decrease in temperature in subaluminous and peraluminous melts, the content of Nb decreases noticeably faster than that of Ta. In this case, the Nb/Ta ratio decreases, respectively, from ~0.6 to ~0.1 in subaluminous and from ~0.45 to ~0.07 in peraluminous melts.

The mutual arrangement of lines of the Ta and Nb concentrations on Figures 1a-c differs significantly if we compare the data obtained at the dissolution of tantalite with the results on the dissolution of columbite from (Chevychelov et al., 2010). At dissolution of tantalite, which contains more tantalum than niobium, the content of Ta in the melt is higher than that of Nb in all melts studied. At the same time, when dissolving columbite, in which niobium predominates over tantalum, the content of Ta in the melt is higher than Nb at T =750 -850°C only in peraluminous melts at A/NKMF index more than 1.5-1.6, and at T =650°C at A/NKMF index more than 0.9 in both subaluminous and peraluminous melts.

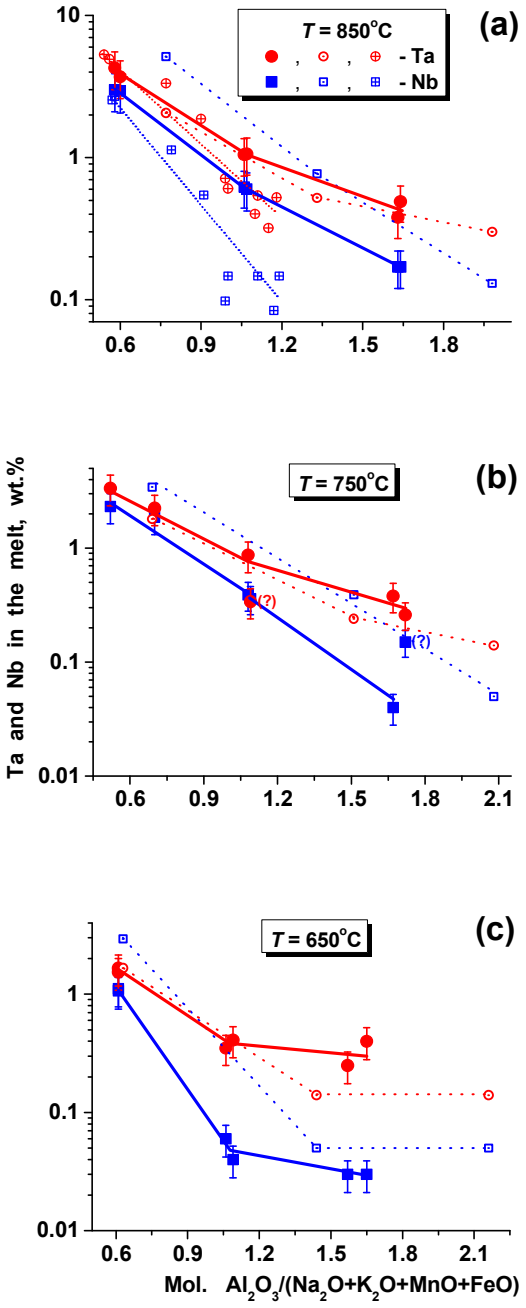

Fig. 1. Effective solubilities of Ta and Nb at the dissolution of tantalite in granitoid melts with different alkalinity - alumina content at P =100 MPa, (a) T =850°C, (b) 750°C, and (c) 650°C (filled symbols, solid lines). For comparison, the results on the dissolution of columbite are shown (Chevychelov et al., 2010; open symbols with dots, dot-and-dash lines), as well as in Fig. 1a experimental data on the dissolution of pure $MnNb_2O_6$ and $MnTa_2O_6$ in granite melts at T =800°C and P =200 MPa (Linnen and Keppler, 1997; open symbols with crosses, dot-and-dash lines).

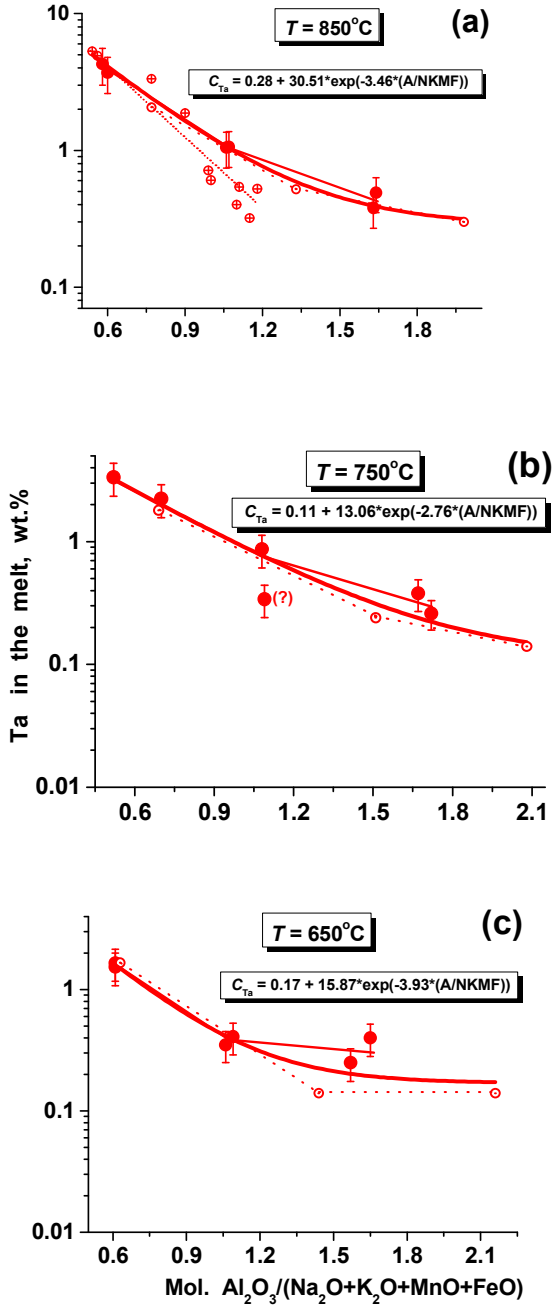

Fig. 2. The approximations by exponential functions the dependences of the effective solubilities of Ta shown in Fig. 1. Calculation formulas are given on the graphs. C_{Ta} is the content of Ta in the melt, A/NKMF is the mol. $Al_2O_3/(Na_2O+K_2O+MnO+FeO)$. Symbols in the caption to Fig. 1.

As shown in Figure 1a at T =850°C and P =100 MPa, the effective solubility of Ta is practically the same when both tantalite and columbite are dissolved in model granitoid melts over the entire studied A/NKMF indexes range from ~0.8 to ~1.6. Moreover, in the alkaline melts (A/NKMF index from ~0.6 to ~0.9), the data on tantalite and columbite are quite close to the data on the solubility of pure tantalite, $MnTa_2O_6$, in model granite melts of different composition at T =800°C and P =200 MPa

(Linnen , Keppler, 1997). Results of all three considered series of experiments were approximated by exponential functions calculated using the OriginPro program. The calculation formulas are shown in Figures 2a-c. As the temperature decreases to 750°C (Fig. 2b), the agreement between the data on tantalite and columbite in alkaline melts (A/NKMF index ~0.7–1.1) is very good, and in the melts enriched with alumina, the Ta concentrations coincide within the error. Finally, at 650°C (Fig. 2c), such the coincidence of data in alkaline melts (A/NKMF index ~0.6 -1.1) is almost perfect, and in alumina-enriched melts, the effective solubility of Ta at dissolution of tantalite is higher than the data obtained at dissolution of columbite (Fig. 2c). Possibly, this is due to the low Ta contents in the melt at these conditions and, therefore, the higher relative errors of the analysis.

The effective solubility of Nb in the melt, in contrast to Ta, varies significantly depending on which mineral, tantalite or columbite, is dissolved in the melt. In the case of the same alkalinity - alumina content of the melt, when dissolving columbite, the concentration of Nb is always higher than when dissolving tantalite. In Figures 1a and 1b, the Nb concentration lines constructed from experiments with tantalite dissolution are located below and parallel to those lines from experiments with columbite dissolution.

Funding. This study was carried out under government-financed research project *of IEM RAS No.* FMUF-2022-0004 and FMUF-2022-0003.

References

Chevychelov V.Yu., Borodulin G.P., Zaraisky G.P. Solubility of Columbite, $(Mn,Fe)(Nb,Ta)_2O_6$, in Granitoid and Alkaline Melts at 650–850°C and 30–400 MPa: An Experimental Investigation // Geochemistry International. 2010. V. 48. No 5. P. 456-464.

Linnen R.L., Keppler H. Columbite solubility in granitic melts: consequences for the enrichment and fractionation of Nb and Ta in the Earth's crust // Contrib. Mineral. Petrol. 1997. V. 128. P. 213-227.